Available online at www.sciencedirect.com
SCIENCE DIRECT®
Journal of Nuclear Materials 346 (2005) 165–184
journal of nuclear materials
www.elsevier.com/locate/jnucmat

Tensile properties and fracture mode of a wrought ODS molybdenum sheet following fast neutron irradiation at temperatures ranging from 300 °C to 1000 °C

B.V. Cockeram [a,*], R.W. Smith [a], L.L. Snead [b]

[a] Bettis Atomic Power Laboratory, Bechtel-Bettis, Inc., P.O. Box 79, West Mifflin, PA 15122-0079, USA
[b] Oak Ridge National Laboratory, P.O. Box 2008, Oak Ridge, TN 37831-6138, USA

Received 8 February 2005; accepted 10 June 2005

Abstract

A commercially available wrought oxide dispersion strengthened (ODS) molybdenum alloy was irradiated in the high flux isotope reactor (HFIR) at 294–936 °C to neutron fluences between 2.28 and 24.7×10^{25} n/m^2 ($E > 0.1$ MeV) or (1.2–13.1 dpa-Mo). Irradiation of ODS molybdenum at 300 °C and 600 °C results in large increases in strength (57–173%). The DBTT for 300 °C-irradiated ODS Mo was 800 °C, which is the same as observed for low carbon arc cast (LCAC) and TZM molybdenum irradiated to the same dose. The DBTT for 600 °C-irradiated ODS Mo was room-temperature, which is a significant improvement over the DBTT values determined for LCAC (300 °C) and TZM (700 °C) and from literature data. The micro-structural feature of small, elongated grains likely enhances the resistance of ODS to irradiation embrittlement. Irradiation of ODS Mo at 870–1000 °C resulted in small increases in yield strength (10–34%) with a post-irradiated DBTT comparable to non-irradiated material (−100 °C).

1. Introduction

Molybdenum is a refractory metal that undergoes no phase change from ambient to the relatively high melting temperature of 2610 °C. The high strength and creep-resistance at high temperatures, high thermal conductivity, and measurable tensile ductility of molybdenum are desired properties for many advanced applications [1–7]. Improvements in the high-temperature strength and creep resistance of molybdenum, such as commercially available unalloyed low carbon arc cast (LCAC) molybdenum, have been achieved by alloying to produce solid-solution and precipitation strengthening [8–12]. Commercially successful examples of these approaches are molybdenum–rhenium alloys, which involve solid-solution strengthening, and TZM molybdenum, which involves both carbide precipitate and solid-solution strengthening. An oxide dispersion strengthened (ODS) molybdenum alloy has been developed that possesses improved creep resistance when the material is highly worked to produce a fine dispersion of La-oxide particles, a fine grain size (≈1.2 μm), and a high recrystallization temperature (1700 °C) [13–18]. The addition of oxide particles also limits grain

DOI of original article: 10.1016/j.jnucmat.2005.06.016
* Corresponding author. Tel.: +1 412 476 5647; fax: +1 412 476 5779.
E-mail address: cockeram@bettis.gov (B.V. Cockeram).

0022-3115/$ - see front matter © 2005 Elsevier B.V. All rights reserved.
doi:10.1016/j.jnucmat.2005.06.020

growth and stabilizes a fine grain size. High amounts of tensile ductility are typically observed for molybdenum-base alloys at low temperatures when the grain size is fine, the oxygen content is low, and the ratio of carbon to oxygen is high [8,9,19–23]. The high tensile ductility, high fracture toughness, and low ductile to brittle transition temperature (DBTT) of ODS molybdenum is thought to result from its very fine grain size [17,18]. Since wrought processing results in alignment of the grains and oxide particles in the working direction, the mechanical properties of ODS molybdenum are anisotropic, but are generally an improvement over many molybdenum-base alloys.

Irradiation of most commercially available molybdenum alloys at temperatures as high as 600 °C typically results in the formation of a high number density ($>10^{19}$ m^{-3}) of dislocation loops and/or voids that increase the flow stress of the material to levels that are higher than the inherent fracture stress and results in brittle failure [1–6]. This irradiation embrittlement is characterized by an increase in the DBTT. The Stage V recovery temperature for prominent vacancy diffusion in molybdenum is 600 °C, which explains why susceptibility to embrittlement starts to diminish for temperatures above 600 °C. However, the kinetics for micro-structural evolution of the defects that restrict dislocation motion can be slow at this temperature, which can result in embrittlement being observed at irradiation temperatures as high as 800 °C in some cases. Given that the nucleation and growth of voids, loops and other defect clusters that impede dislocation flow depend on point defect transport, it is expected that barrier formation can be influenced by careful control of pre-existing micro-structural sinks [1–7,24]. The fine grain size and fine oxide particle dispersion of ODS molybdenum are micro-structural features that may result in improved resistance to irradiation embrittlement, but the influence of these features on irradiation effects has received little attention [29]. The purpose of this work is to determine the change in the tensile properties of wrought ODS Mo sheet following irradiation in the high flux isotope reactor (HFIR) at 300 °C, 600 °C, and 870–1000 °C to neutron fluences between 2.28 and 24.7×10^{25} n/m^2 ($E > 0.1$ MeV).

2. Materials and experimental procedure

Wrought ODS molybdenum sheet (0.76 mm thick) was obtained from H.C. Starck, Inc. with the composition provided in Table 1. Glow Discharge Mass Spectrometry (GDMS) results from Shiva Technology were generally within a factor of two of the chemical certification with the exception of oxygen, which likely resulted from the oxide particles nominally (2 vol.%) present in the material. The processing of ODS molybdenum has been described [13–18], and basically consists of wet doping Mo-oxide powder with a La-nitrate solution, pyrolyze to form a fine dispersion of La-oxide in molybdenum powder, consolidation of the powder, and wrought processing to form a sheet followed by a stress-relief anneal in vacuum at 1200 °C/1 h. A sub-sized SS-1 flat tensile geometry [7] was used in this work with a nominal size of 44.45 mm long × 4.95mm wide with a 20.32×1.52 mm gauge length and nominal thickness of 0.76 mm. The tensile specimens were machined in the longitudinal stress-relieved (LSR) or transverse stress-relieved (TSR) condition, and then laser scribed for identification, electropolished, and again given a stress-relief anneal in vacuum at 1200 °C for 1 h.

Capsule designs used to irradiate the ODS Mo tensile specimens were comparable to those from previous work [7,23]. One capsule consisted of eight tensile specimens that were loaded into a holder, which was a rectangular axial opening machined into a cylinder (5.08 cm diame-

Table 1
Chemical analysis of the ODS sheet (in weight ppm) from the material certification reports and determined from GDMS analysis at Shiva Technology

Material/Lot#	C	O	N	Ti	Zr	Fe	Ni	Si	La[2]	Al	Ca	Cr	Cu	Other
ODS Sheet ODS Mo Ingot 32438 Heat# LA 23795 0.76 mm sheet	40	NA	NA	<10	NA	27	<10	<10	1.08 wt%	<10	<10	<10	<10	<10 Mg <10 Pb <10 Sn
GDMS data ODS Sheet ODS Mo Ingot 32438 Heat# LA 23795	~0.5	~3100	~3.8	<5	0.1	48	7.4	1.6	9800	4.2	5.2	19	3.1	3 Mg 7.5 K 150 W

Note: 1. All material was obtained from H.C. Starck, which was formally known as CSM Industries, Inc., Cleveland, OH. 2. La content is given in wt%, all other compositions are reported in ppm. 3. NA = Not available. 4. Trace GDMS composition for elements not listed was <1 ppm.

ter × 5.6 cm long). Aluminum holders were used for the 300 °C irradiation and vanadium was used for the 600 °C and 1000 °C irradiations. The capsules were welded to seal an inert helium atmosphere in each capsule. The tensile holders were centered within the capsule using a thimble. A thermal model was used to determine the irradiation temperatures, which was set by the size of the gas-gap between the holder/capsule. Thermal calculations show that the maximum temperature gradients through the tensile specimens were 10 °C and 15 °C for the radial and axial direction, respectively, at a target irradiation temperature of 300 °C and on the order of 25 °C in either direction for the 600–1000 °C target irradiation temperatures. The irradiation temperatures were verified by using passive silicon carbide (SiC) temperature monitors [7,25]. Analysis of the temperature monitors indicates that the irradiation temperature was within 50 °C or less of the target irradiation temperatures reported in Table 2 for target irradiation temperatures of 300 °C and 600 °C (actual irradiation temperature of 294 °C and 560–609 °C, respectively), and within ±100 °C or better for irradiations at the target temperature of 968–1000 °C (actual irradiation temperatures of 870 °C and 936 °C) [7]. The one exception is for the f3 capsule, where the nominal irradiation temperature was found to be 784 °C. It is not clear at this time why this deviation in temperature occurred, and at what point in the irradiation test the temperature deviation occurred [42].

Irradiations were performed in the peripheral target tube position (PTP) of the high flux isotope reactor (HFIR) in one to ten cycles at 85 MW of power (Table 2). The capsules or specimens were not shielded from the spectrum produced by HFIR, which results in an estimated nominal peak fast neutron flux of 10×10^{18} n/m^2 s ($E > 0.1$ MeV), and a peak thermal neutron flux of 2.2×10^{19} n/m^2 s ($E < 0.1$ MeV). The displacement damage produced by irradiation was determined to be primarily the result of the fast flux. Reactions that result from thermal neutron absorption are not thought to be a significant contribution to irradiation damage [7,23]. The maximum fluence values reported in Table 2 (3.8–12.4 dpa) are calculated to produce a very low concentration (<0.2 and 0.6 wt%) of transmutation products that are primarily Tc and Ru with 3–4 ppm amounts of Zr and Nb [7,23,26]. This concentration of transmutation products was independently confirmed using a point depletion program. The changes in tensile properties are expected to result from the defects produced by irradiation. Transmutation products are not believed to have a measurable effect on the tensile results.

All tensile tests were performed at temperatures ranging from −150 °C to 1000 °C at an actuator displacement rate of 0.017 mm/s (strain rate = 0.00083 min^{-1}) in accordance with ASTM E8 [27]. Specimen load and crosshead displacement were recorded and used to determine the tensile properties in terms of engineering stress/strain. No correction was made for the compliance of

Table 2
Estimated irradiation temperature, neutron fluence, and calculated DPA values for ODS molybdenum following irradiation in HFIR

Target irradiation temperature [°C]	Actual irradiation temperature[2] [°C]	Capsule number	Irradiation cycles	Neutron fluence [$E > 0.1$ MeV], $\times 10^{25}$ n/m^2/(estimated molybdenum dpa)[3]		
				2.28	6.44–7.26	23.2–24.7
300[1]	294	F1 and f2	388–397[4]	N/A	N/A	23.2/(12.3)
600[1]	609	N1	388–390[4]	N/A	7.26/(3.9)	N/A
600[1]	560	F4	388–397[4]	N/A	N/A	24.6/(13.1)
600[1]	784	F3	388–397[4]	N/A	N/A	24.6/(13.1)
968[1]	870	K1	380[5]	2.28/(1.2)	N/A	N/A
968[1]	870	K2	380–382, 372C[5]	N/A	6.44/(3.4)	N/A
1000[1]	936	F5 and F6	388–397[4]	N/A	N/A	24.7/(13.1)

Notes: 1. The target irradiation temperature was the aim calculated tensile specimen temperature that was designed for the irradiation test. The irradiation temperatures were generally within ± 50 °C for irradiations at 300 °C and 600 °C, and ± 100 °C for irradiations performed at 1000 °C. 2. Analysis of passive temperature monitors has confirmed these irradiation temperatures. 3. The conversion from neutron fluence to molybdenum DPA for the HFIR spectrum was determined using SPECTER [28]. 4. Two sets of irradiations were performed. These irradiations were performed over a period of 26 July 2002–17 November 2003. Cycles 388, 389, and 390 were used to produce a neutron fluence of 72.6×10^{24} n/m^2. The MW days and hours of operation for each cycle are as follows: cycle 388 (2094 MW days and 591.2 h), cycle 389 (2124 MW days and 599.7 h), cycle 390 (2111 MW days and 596.1 h), cycle 391 (2090 MW days and 590.0 h), cycle 392 (2077 MW days and 586.5 h), cycle 393 (2143 MW days and 605.0 h), cycle 394 (2130 MW days and 601.3 h), cycle 395 (2198 MW days and 620.6 h), cycle 396 (2203 MW days and 621.9 h), cycle 397 (2216 MW days and 625.8 h). 5. Two sets of irradiations were performed. These irradiations were performed over a period between 15 June 2000 and 1 October 2000. Only cycle 380 was used to produce the neutron fluence of 22.8×10^{24} n/m^2. The MW days and hours of operation for each cycle are as follows: cycle 380 (2230 MW days and 629.6 h), cycle 381 (2123 MW days and 599.4 h), cycle 372C (302 MW days and 85.3 h), and cycle 382 (1755 MW days and 495.5 h). 6. N/A indicates that irradiations were not performed at these conditions.

the load train for the stress–strain curves, and all stress and strain data are calculated from the raw load–displacement results [7]. Room-temperature tests were conducted at atmospheric pressure, while tests at elevated temperatures were performed in a vacuum furnace ($< 6 \times 10^{-5}$ MPa) that was equipped with refractory-metal heat shields and elements. Heating to the test temperature was achieved in 30–45 min with a hold time of 30 min prior to testing. Testing at sub-ambient temperatures was accomplished in a controlled chamber using nitrogen gas to cool to −50 °C to −150 °C [7]. Determination of the tensile DBTT was primarily based on fractographic examinations that were performed using a scanning electron microscope (SEM).

3. Results and discussion

3.1. Unirradiated tensile properties

Tensile properties for unirradiated ODS molybdenum (Mo) are summarized in Table 3. The grain structure of ODS Mo is shown in Fig. 1 to consist of elongated, sheet-like pancaked grains that are aligned in the working direction with La-oxide ribbon and fine particles that are also aligned in the working direction and are frequently at grain boundaries and within grains [14–17,29]. Measurements of the grain size show in Table 4 that the grain dimensions were thinner and longer in the longitudinal orientation. Lower tensile strength and

Table 3
Summary of unirradiated tensile data for ODS molybdenum sheet

Test temperature [°C]	Tensile strength [MPa]		Tensile ductility [%]			Strain hardening exponent, n
	Ultimate tensile stress	0.2% Yield stress	Total elongation	Uniform elongation	Reduction in area	
Longitudinal stress-relieved						
−194	1612.7	1612.7	0	0	0	–
−150	1451.3 ± 162.3	1489.7 ± 137.9[2,3]	0.4 ± 0.3	0.2 ± 0.2	1 ± 1	–
−100	1229.3 ± 84.0	1240.7 ± 104.8[2,3]	6.1 ± 2.4	0.9 ± 0.6	32 ± 14	−0.064
−50	1000.7 ± 53.6	965.1 ± 55.8	14.2 ± 2.6	4.0 ± 3.1	45 ± 8	0.036
22	794.1 ± 24.5	735.1 ± 32.6	20.6 ± 3.7	9.4 ± 3.2	53 ± 9	0.067
150	698.5 ± 68.3	614.3 ± 32.2	18.6 ± 2.5	9.7 ± 0	54 ± 1	0.098
201	669.5	574.4	17	11	63	–
300	570.7 ± 28.1	511.6 ± 19.7	9.7 ± 3.9	4.9 ± 2.9	64 ± 1	–
400	561.3	479.9	10	8	64	–
600	485.1 ± 16.2	445.6 ± 19.8	4.3 ± 0.4	0.9 ± 0.3	70 ± 4	0.086
700	404.0 ± 88.7	373.4 ± 85.3	4.4 ± 0.6	1.5 ± 0.6	70 ± 1	0.078
800	422.7 ± 35.1	419.9 ± 1.0	4.7 ± 0.5	1.6 ± 0.6	77 ± 0	0.064
982	360.1 ± 32.9	346.7 ± 35.5	5.6 ± 0.9	0.9 ± 0.2	70 ± 11	–
1000	364.7 ± 8.8	339.2 ± 3.9	7.2 ± 0.3	1.2 ± 0.2	78	−0.006
1200	197.2	182.7	12	1	85	–
1400	128.2	113.8	15	1	66	–
1600	61.4	61.4	19	3	32	–
1700	53.8	40.6	11	3	20	–
Transverse stress-relieved						
−194	1137.0	1137.0	0	0	0	–
−150	1228.0	1228.0	< 1	0	0	–
−100	1315.4 ± 43.7	1318.5 ± 45.4[2,3]	0.9 ± 0.7	0.4 ± 0.1	10 ± 9	–
−50	1099.5 ± 13.8	1106.2 ± 28.0[2,3]	6.0 ± 1.1	0.5 ± 0	6 ± 6	–
22	827.7 ± 26.5	823.5 ± 34.3	9.6 ± 2.0	3.8 ± 1.8	9 ± 3	–
150	693.6	610.2	10	5.2	–	–
200	624.2 ± 11.6	548.8 ± 21.2	6.3 ± 2.4	3.6 ± 1.2	14	–
300	574.8 ± 5.8	517.6 ± 7.6	4.2 ± 0.3	2.9 ± 1.0	22 ± 1	–
400	524.2 ± 3.5	478.5 ± 12.5	3.2 ± 0.7	2.5 ± 1.3	27 ± 4	–
982	265.5	245.5	4	1	63	–
1200	165.5	151.7	9	2	74	–
1400	73.8	53.8	25	6	26	–
1600	48.3	41.4	18	9	13	–

Note: 1. '–' means that a value was not measured for this condition. 2. An upper/lower yield point is observed. 3. A slight yield point is observed, resulting in a higher yield strength than the ultimate strength, or the yield strength being equivalent to the ultimate tensile strength. 4. For cases where more than one data point were determined at a given test temperature, the average ± the standard deviation is reported.

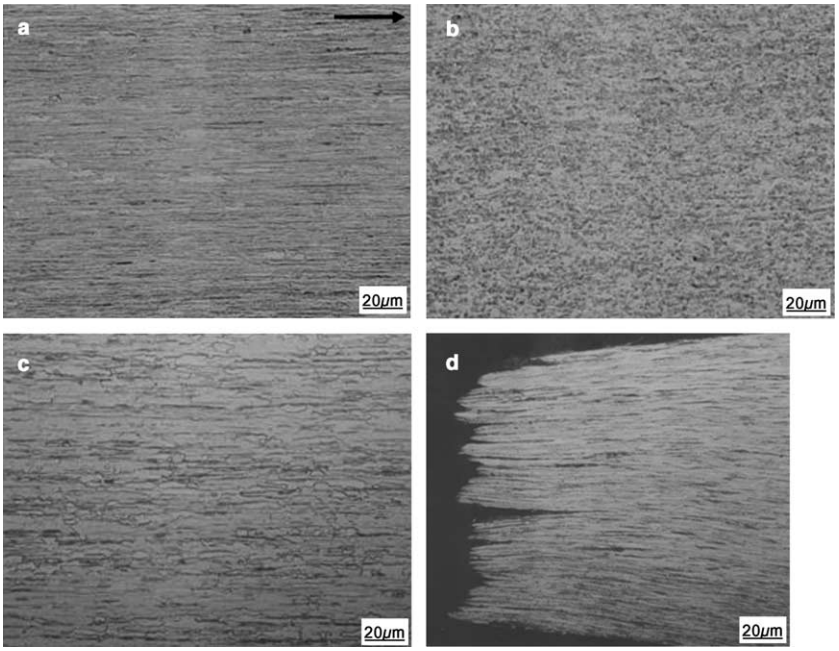

Fig. 1. Polished and etched optical micro-graphs of the micro-structure of stress-relieved ODS molybdenum sheet: (a) longitudinal orientation, (b) transverse orientation, (c) surface of sheet, and (d) longitudinal orientation near fracture surface of specimen tested at room-temperature. A Murakami etch was used, with the arrow identifying the longitudinal direction.

Table 4
Summary of grain size measurements for ODS sheet

Alloy	Grain diameter [μm]		Grain length [μm]	
	Average	Standard deviation	Average	Standard deviation
ODS sheet – LSR	1.2	0.8	45.7	25.0
ODS sheet – TSR	2.5	1.0	33.3	12.1
[1]LCAC Sheet – LSR[1]	3.9	2.5	172	79
LCAC Sheet – TSR[1]	5.0	2.7	78.1	38.2
TZM Plate – LSR[1]	3.9	2.5	273	105
TZM Plate – TSR[1]	6.1	3.8	132	69

1. Results for LCAC and TZM are reported in [42].

higher elongation values were observed in the longitudinal orientation, which is consistent with literature data for ODS Mo [13–17]. The presence of more grain boundary and oxide interface area in the TSR orientation results in a higher fraction of boundaries and results in increased strength in the transverse orientation, but fracture initiation typically occurs at grain boundaries, which results in a lower tensile elongation for TSR ODS Mo relative to LSR. The oxide particles limit grain growth, result in a high recrystallization temperature of 1700 °C for 1 h heat treatments, and result in a much finer grain size.

The stress–strain curves for ODS Mo show in Fig. 2 that a low work hardening rate, or strain hardening exponent of $n = 0.098$ to -0.064 (Table 3), is observed that is consistent with the literature data for commercial molybdenum alloys [7,13–17,30–39]. These stress–strain curves were not corrected for the compliance of the load train. The fracture surfaces for LSR ODS Mo tested at −100 °C are shown in Fig. 3(a) to consist of a ductile laminate failure mode, where fracture initiation occurs at grain boundaries and oxide interfaces in the region of triaxial stresses to produce separation of the microstructure into laminate type grains that are then pulled to fracture with a high degree of necking (Fig. 1(d)); this is also known as thin sheet toughening [17,18,40–42]. Transgranular cleavage (Fig. 3(b)) and nil amounts of ductility were observed for LSR ODS Mo tested at

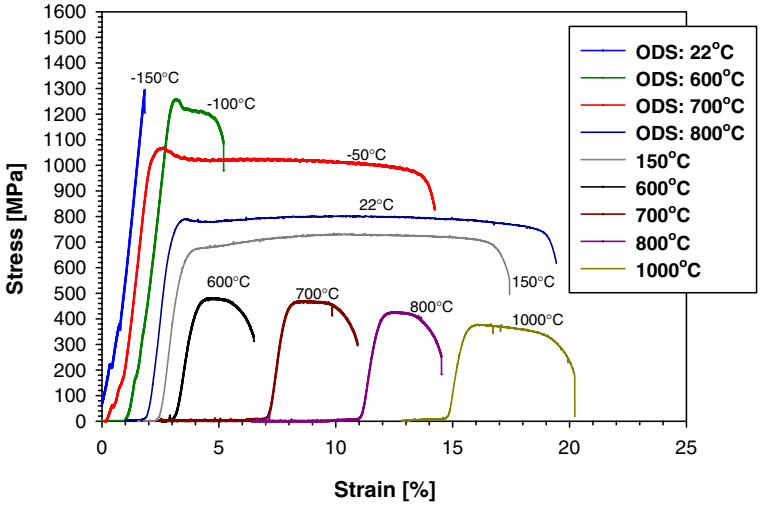

Test Temp	-100°C	-50°C	22°C	150°C	600°C	700°C	800°C	1000°C
n	-0.064	0.036	0.067	0.098	0.086	0.078	0.064	-0.006

Fig. 2. Load–displacement curves for non-irradiated ODS molybdenum in the LSR condition. The strain hardening exponent data provided below are summarized in Table 3. The stress–strain data were determined from the raw load–displacement results, and no correction was made for the compliance of the load frame.

−150 °C. The large amount of ductility (total elongation and Reduction in Area (RA)), plasticity observed in the stress–strain curves, and ductile failure mode observed for LSR ODS Mo at −100 °C with brittle failure observed at −150 °C indicate that the DBTT was higher than −150 °C and lower than −100 °C, but is conservatively defined as −100 °C, see Table 5. Large amounts of tensile ductility, plasticity in the load–displacement curves and evidence for a ductile failure mode were consistently observed for TSR ODS Mo at room-temperature, while low ductility and brittle failure modes were observed at −50 °C. Table 5 shows that the DBTT for TSR ODS Mo was conservatively defined as room-temperature.

3.2. Post-irradiation tensile properties for irradiation at 294 °C and 560–609 °C

3.2.1. Results for longitudinal stress-relieved (LSR) ODS

All post-irradiated tensile data for LSR ODS Mo are summarized in Table 6. Large increases in tensile strength and large amounts of irradiation hardening, which are reflected by the increase in yield strength, are observed for irradiation at 294 °C and 560–609 °C in Fig. 4(a) with increases ranging from 57% to 173%. These large increases in tensile strength are within the range of literature data, but are generally at the upper bound of post-irradiated tensile strength for molybdenum alloys [1–7,30–39,42–44]. All tensile strength values determined at temperatures less than the DBTT are actually a fracture stress. In the brittle regime the material fractures before yielding. Scatter in the size and distribution of pre-existing flaws has been observed to result in large variation of the fracture strength values determined for LCAC and TZM molybdenum irradiated under the same conditions [42]. However, little scatter in the LSR ODS Mo tensile strength values was observed for the 294 °C and 560 °C irradiations, and the values are generally similar.

The notable exception to the similarity in irradiation hardening results for the 294 °C and 560–609 °C irradiations is that exceptionally low tensile strength and high ductility were observed for one capsule (f3) that was intended for a 600 °C irradiation [42]. All specimens irradiated in capsule f3 exhibited tensile properties and change in electrical resistivity results that were comparable to values for 1000 °C irradiations. Analysis of temperature monitors also confirmed that the last nominal irradiation temperature for capsule f3 was 784 °C, and was possibly close to 1000 °C for some period of time, see Table 2. If irradiation of capsule f3 actually occurred for some time at 600 °C and then the irradiation temperature was increased to 784 °C for some time, these results indicate that irradiation at high temperatures results in the recovery of the defect structure that results in irradiation hardening. The data for specimens irradiated in capsule F3 are listed in Table 6. Further discussion of results from the f3 capsule is not pursued.

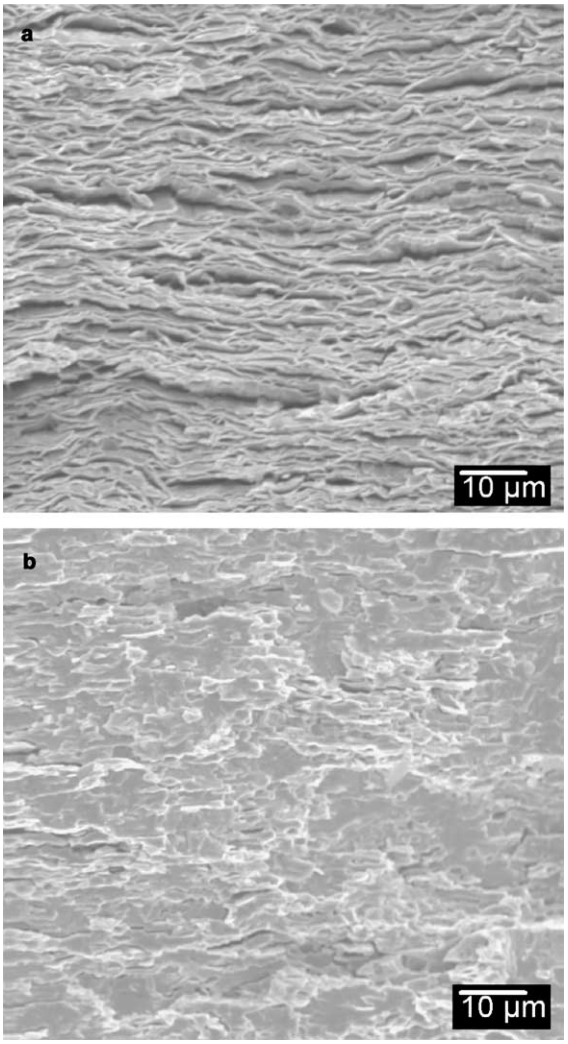

Fig. 3. SEM fractography of non-irradiated LSR ODS molybdenum following tensile testing at: (a) temperature of −100 °C showing a ductile-laminate failure, and (b) temperature of −150 °C showing a transgranular cleavage failure mode.

The tensile strength and irradiation hardening values determined for 294 °C and 560–609 °C irradiated LSR ODS Mo when tested at room-temperature to 300 °C were slightly higher than results determined at a comparable test temperature for TZM and LCAC [3,42]. Tensile strength results determined for 294 °C and 560–609 °C irradiated ODS Mo exhibit a stronger dependence on test temperature than results obtained for commercial molybdenum alloys such as TZM and LCAC [42], and the tensile strength results for 294 °C and 560–609 °C irradiated LSR ODS Mo at test temperatures ranging from 600 °C to 800 °C are generally lower than for TZM and LCAC. Strong changes in tensile results with test temperature and similarity in tensile results for specimens irradiated at 294 °C and 560–609 °C can be explained by the differences in fracture mechanisms, as discussed in the following section. The tensile strength and irradiation hardening results for the 560–609 °C irradiations at a dose of 24.6×10^{25} n/m^2 (13.1 dpa-Mo) and 7.26×10^{25} n/m^2 (3.9 dpa-Mo) are shown in Fig. 4(a) to be comparable. This indicates that saturation of irradiation hardening for the 560–609 °C irradiations of LSR ODS Mo occurs at a fluence at or below 7.26×10^{25} n/m^2 (3.9 dpa-Mo), which is the same as observed for TZM [42].

For LSR ODS Mo irradiated at 294 °C, low amounts of tensile ductility (Fig. 4(b)) and linear–elastic relationship in the load–displacement curves to failure are shown in Fig. 5(a) at test temperatures between room-temperature and 700 °C. A brittle failure mode of transgranular cleavage was observed at room-temperature (Fig. 6(a)), which was similar to non-irradiated LSR ODS Mo tested at −150 °C (Fig. 3(b)). Although no ductility was observed for the 294 °C irradiated LSR ODS Mo tensile specimens tested at 600 °C and 700 °C, mixed-mode failures that consist of primarily transgranular cleavage with local regions of ductile laminate failure are shown in Fig. 6(b). The mixed-mode failures with ductile laminate features observed at 600 °C and 700 °C, where no tensile ductility was measured, suggest that higher amounts of energy may be absorbed during fracture compared to room-temperature testing, which could only be resolved by measurements of fracture energy such as obtained using a fracture toughness or Charpy test. Measurable amounts of tensile ductility, plasticity in the load–displacement curve, and a ductile failure mode (Fig. 6(c)) were observed for 294 °C irradiated LSR ODS Mo at a test temperature of 800 °C. This indicates that the tensile DBTT was higher than 700 °C and no more than 800 °C, but was conservatively defined as 800 °C (Table 5). The ductile failure mode observed for 294 °C irradiated LSR ODS Mo at 800 °C is characterized by a plastic instability with prompt yielding, a significant decrease in the strain-hardening exponent, and decrease in uniform elongation, which is a typical result observed for the irradiation of metals at low temperatures [45–47], and is similar to that observed at 800 °C for LCAC and TZM Mo irradiated at 300 °C [7,42]. Tensile DBTT values of 800 °C were also observed for LCAC and TZM irradiated at 294 °C to the same dose [42]. However, the fracture surface for 294 °C irradiated LSR ODS Mo was observed to have a higher density of ductile laminate features with a finer laminate spacing, which likely results from a finer grain size and could indicate that more fracture energy is being absorbed.

For the irradiations of LSR ODS Mo at 609 °C to a fluence of 7.26×10^{25} n/m^2 or 3.9 dpa-Mo (Fig. 4), low tensile ductility, linear elastic behavior with no plasticity, and a brittle failure mode consisting of transgranular

Table 5
Summary of pre- and post-irradiation DBTT values determined from tensile testing for ODS molybdenum following irradiation in HFIR to a maximum fluence of 23.2–24.7 × 10^{25} n/m^2, $E > 0.1$ MeV

Alloy/condition	Pre-irradiation DBTT (°C)	Post-irradiated DBTT for irradiation at various irradiation temperatures		
		294 °C	560–609 °C	870–936 °C
ODS – LSR	−100	800 °C	25 °C	−100 °C
ODS – TSR	25	N/A	>25 °C	<300 °C
LCAC – LSR[3]	−100	800 °C	300 °C	−50 °C
LCAC – TSR[3]	−100	N/A	N/A	<25 °C
TZM – LSR[3]	−50	800 °C	700 °C	−50 °C
TZM – TSR[3]	−50	N/A	700 °C	<0 °C

Note: 1. For pre-irradiation DBTT values, the result is based on a ductile failure observed at −100 °C with a brittle failure observed at −150 °C. 2. Post-irradiated DBTT values for 294 °C irradiations (800 °C) are based on a ductile failure observed at 800 °C with a brittle failure observed at 700 °C. For 609–560 °C irradiations, the 25 °C DBTT for LCAC is based on a ductile failure observed at room-temperature and brittle failure observed at −50 °C. For 936 °C irradiations, the −100 °C DBTT is based on a ductile failure observed at −100 °C with a brittle failure mode observed at −150 °C. 3. The results for LCAC and TZM (irradiated to the same dose as ODS) are reported in [42].

cleavage (Fig. 7(a)) was observed for specimens tensile tested at −50 °C. Measurable tensile ductility, plasticity in the load–displacement curves (Fig. 5(b)) and a ductile laminate failure mode similar to non-irradiated material (Fig. 7(b)) were observed at test temperatures equal to or greater than room-temperature. This indicates that the DBTT of LSR ODS Mo irradiated at 609 °C to a dose of 7.26 × 10^{25} n/m^2 (3.9 dpa-Mo) is higher than −50 °C and less than or equal to room-temperature, but is conservatively defined as room-temperature. The tensile results and ductile laminate failure mode observed for LSR ODS Mo irradiated at 560 °C to a higher dose of 24.6 × 10^{25} n/m^2 (13.1 dpa-Mo) and tested at room-temperature (Fig. 7(c)) and 150 °C are essentially comparable to results determined at the lower dose, with the exception of slightly lower ductility and increased strain-hardening rate at the higher dose. These minor differences may represent data scatter for these limited data sets rather than true differences in tensile properties between the higher and lower dose 600 °C irradiations for ODS Mo. These results show that saturation of the change in tensile properties and increase in tensile DBTT from −100 °C to room-temperature is observed for 560–609 °C irradiated LSR ODS Mo at a dose of 7.26 × 10^{25} n/m^2 (3.9 dpa-Mo) or lower with no further change after a higher dose of 24.6 × 10^{25} n/m^2 (13.1 dpa-Mo).

The DBTT values reported in literature for molybdenum irradiated near temperatures of 300 °C [30,39,48] were less than the 800 °C DBTT that was determined for 294 °C irradiated LSR ODS molybdenum (Fig. 8); this is explained by the significantly lower dose for the literature data [42]. Although the DBTT for 294 °C irradiated LSR ODS Mo is comparable to that determined for LCAC and TZM Mo irradiated at 294 °C to the same dose of 23.2 × 10^{25} n/m^2 (Table 5), irradiation of LSR ODS Mo at 560–609 °C results in a DBTT (room-temperature) that is much lower than the DBTTs for LCAC and TZM and is below the range of DBTT values reported in literature for 600 °C irradiations (100–700 °C), see Fig. 8. This result shows that LSR ODS Mo irradiated at 560–609 °C has some resistance to irradiation embrittlement as shown by the room-temperature DBTT.

The fine-grained and elongated, sheet-like grain structure of ODS Mo is one possible reason for this resistance to irradiation embrittlement. Unalloyed molybdenum with a remarkably low interstitial content (30 ppm carbon + 5 ppm oxygen) and an elongated, sheet-like grain structure with small grains (about 2 μm) was also reported in literature [24] to have resistance to irradiation embrittlement with a room-temperature DBTT following irradiations at 373 °C, 519 °C, and 600 °C to neutron fluences between 1.97 and 9.46 × 10^{26} n/m^2 (6.8–34 dpa-Mo). Companion specimens from this high-purity molybdenum results reported in literature [24] were also recrystallized prior to irradiation to form a large grain size (about 20 μm), and brittle fractures were observed for these samples at room-temperature, which indicates that the DBTT for large-grained recrystallized material was above room-temperature. One inconsistency in the reported data for this fine-grained, high-purity molybdenum [24] is that a DBTT above 400 °C was observed in one case for irradiation at 406 °C. The ODS Mo used in this work has a fine grained, elongated sheet-like grain structure with oxide particles, while the high-purity molybdenum also had a fine-grained, elongated sheet-like grains with a low carbon and oxygen content; the common feature was the fine grained, elongated, sheet-like grain structure. Thus, the elongated grain structure of these wrought alloys is likely responsible for resistance to

Table 6
Summary of irradiated tensile data for ODS molybdenum plate

Irradiation temperature [°C]/capsule	Neutron fluence [n/m^2], [$E > 0.1$ MeV]	Test temperature [°C]	Tensile strength [MPa]		Tensile ductility [%]			Strain hardening exponent, n
			Ultimate tensile stress	0.2% Yield stress	Total elongation	Uniform elongation	Reduction in area	
Longitudinal stress-relieved								
294/F2	23.2×10^{25}	22	1689.3	1689.3[1,4]	0.19	0.19	0	–
294/F1		600	1130.1	1130.1[1]	0.01	0.01	0	–
294/F1		700	982.5	982.5[1]	0.19	0.19	2	–
294/F2		800	657.8	659.9[2]	2.2	0.3	52	−2.44
609/N1	7.26×10^{25}	−50	1669.3	1669.3[1]	0.13	0.11	0	–
609/N1		22	1672.0	1661.7	0.64	0.31	18	0.023
609/N1		22	1625.8	1601.7	0.61	0.61	4	–
609/N1		150	1575.5	1549.3	1.61	1.08	17	0.064
609/N1		300	1434.2	1394.2	1.45	0.09	21	0.11
609/N1		600	1214.2	1110.1	1.14	0.94	10	–
560/F4	24.6×10^{25}	22	1608.6	1587.2	0.64	0.56	8	0.13
560/F4		150	1530.0	1508.6	0.8	0.6	10	0.18
784/F3[5]		−50	1301.8	1301.8[6]	2.5	0.04	52	−0.33
784/F3[5]		600	747.4	712.9	2.5	0.7	60	0.30
870/K1	2.28×10^{25}	−100	1300.4	1365.9[9]	1.2	0.4	33.1	−0.26
870/K1		−50	1003.9	1157.0[9]	11.6	1.3	35.6	0.014
870/K1		22	770.2	829.5[9]	16.3	7.1	53.5	0.048
870/K1		22	750.9	843.3[9]	23.7	11.6	–	–
870/K1		982	320.6	314.4	6.7	2.2	70.6	0.006
870/K1		982	335.8	321.3	8.5	2.6	–	–
870/K2	6.44×10^{25}	−100	1367.3	1486.6[9]	1.4	0.4	38.0	−0.40
870/K2		−50	1183.2	1279.0[9]	2.9	0.5	40.0	−0.21
870/K2		22	887.4	915.0[9]	17.5	11.8	46.7	0.082
870/K2		22	922.6	1011.5[9]	16.0	11.4	–	–
870/K2		982	462.7	466.8[9]	9.0	2.6	61.6	0.022
870/K2		982	475.8	466.8	5.3	2.6	–	–
936/F6	24.7×10^{25}	−150	1803.7	1803.7[1]	0.05	0.05	0	–
936/F5		−100	1506.6	1506.6[2,7]	2.0	0.02	42	−0.61
936/F5		22	903.2	981.2[2,8]	5.2	1.9	59	0.025
936/F6		1000	539.2	521.3	3.3	1.0	34	0.15
Transverse stress-relieved								
609/N1	7.26×10^{25}	22	1306.6	1306.6[1]	0.0	0.0	0	–
870/K1	2.28×10^{25}	300	513.0	513.0	6.6	2.8	30.9	–
870/K1		300	508.9	508.2	10.3	5.0	–	–
870/K2	6.44×10^{25}	300	650.2	669.5	1.4	0.6	25.2	–
870/K2		300	710.2	713.6	3.2	2.3	–	–

Notes: 1. Since the uniform elongation was <0.2%, the yield strength cannot be determined, and is listed as being equal to the ultimate strength. 2. A slight yield point is observed, resulting in a higher yield strength than the ultimate strength, or the yield strength being equivalent to the ultimate tensile strength. 3. '–' means that a value was not measured for this condition. 4. Initial fracture at pinhole followed by a second test shoulder loading. 5. The irradiation temperature for these specimens exceeded 600 °C by a large margin at some point during the irradiation, and was determined to be 784 °C. 6. An upper/lower yield point was observed for this test with values of 1301.1/1155.6 MPa. 7. An upper/lower yield point was observed for this test with values of 1506.6/1339.0 MPa. 8. An upper/lower yield point was observed for this test with values of 981.2/894.3 MPa. 9. A yield point is observed, followed by a lower loads than the initial yield point, resulting in a lower ultimate tensile strength.

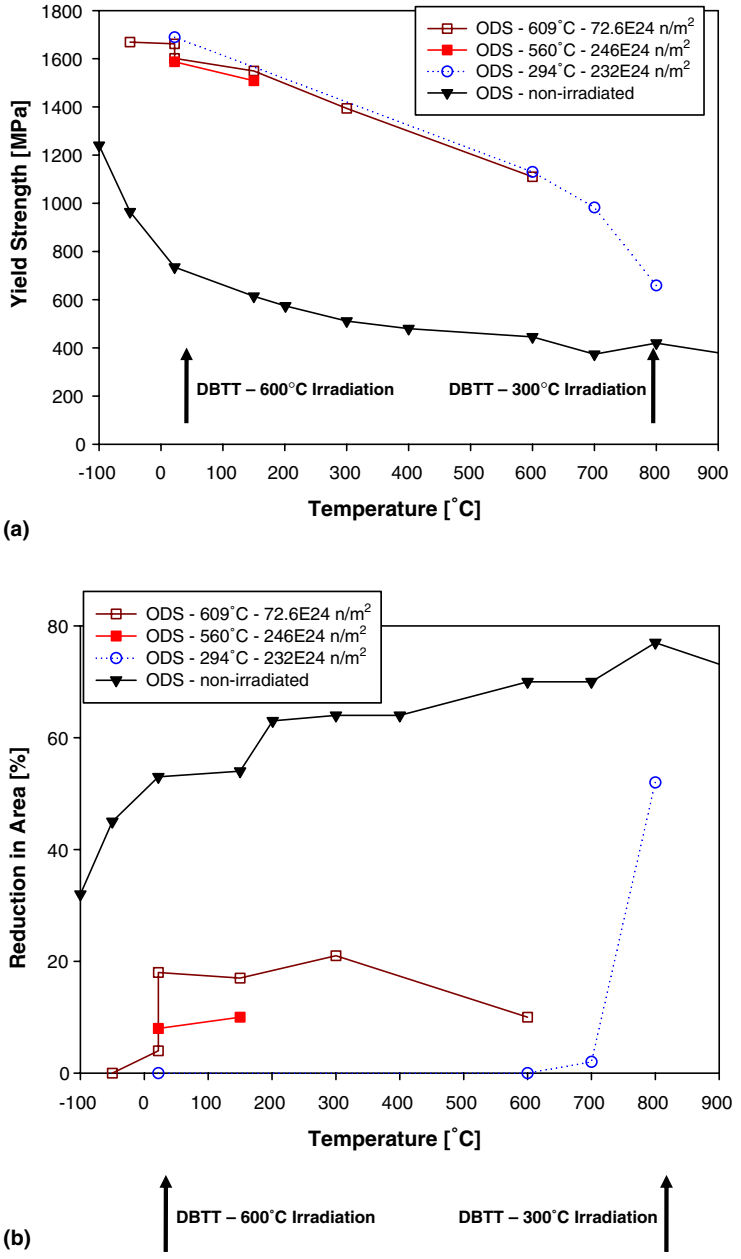

Fig. 4. Comparison of non-irradiated and post-irradiated tensile results for LSR ODS molybdenum following irradiation at 294 °C and 560 °C: (a) yield strength values, and (b) reduction in area values. The tensile strength values determined at temperatures below the DBTT are actually a fracture stress in some cases as true plastic deformation has not been achieved. The fluences of 72.6×10^{25} n/m^2, 23.2×10^{25} n/m^2, and 24.6×10^{25} n/m^2 correspond to a Mo-dpa of 3.9, 12.3, and 13.1, respectively.

irradiation embrittlement. However, the oxide particles present in ODS Mo and the low interstitial content of the high-purity molybdenum may also play an important role in mitigation of irradiation embrittlement. LCAC molybdenum, which also has an elongated, sheet-like grain structure that is slightly coarser than ODS, has a DBTT of 300 °C, which is an improvement over the 700 °C DBTT observed for TZM [42]. The slightly coarser grain size and higher carbon content of LCAC (90 ppm) may explain why the DBTT is not as low as observed for ODS Mo, and could also indicate that the oxide particles present in ODS Mo are further

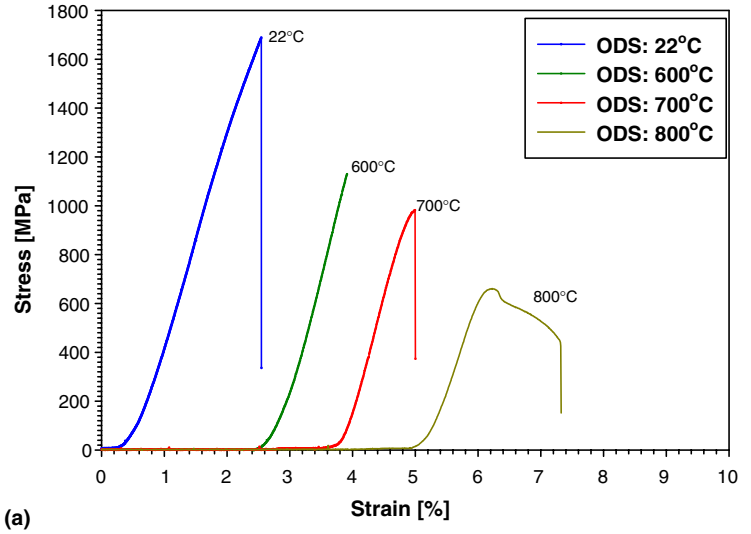

Test Temp	22°C	600°C	700°C	800°C
n	--	--	--	-2.44

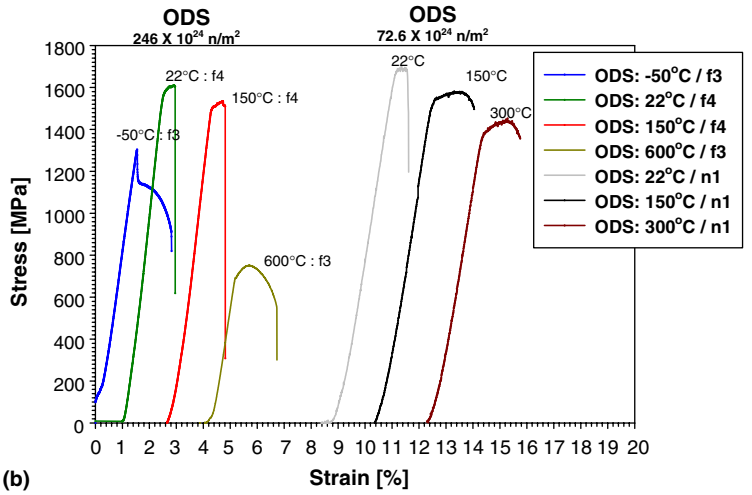

Capsule	f4		f3		n1		
Test Temp	22°C	150°C	-50°C	600°C	22°C	150°C	300°C
n	0.13	0.18	-0.33	0.30	0.023	0.064	0.11

Fig. 5. Plot of load–displacement curves for LSR ODS molybdenum tested a temperatures between −50 °C and 800 °C after irradiation at: (a) 294 °C, and (b) 560–609 °C. For the case of the 560 °C irradiations to a fluence of 24.6×10^{25} n/m^2, the capsule is noted as either f4 (560 °C irradiation temperature) and f3 (nominal irradiation temperature of 784 °C), while capsule n1 609 °C irradiations had a dose of 7.26×10^{25} n/m^2. The stress–strain data were determined from the raw load–displacement results, and no correction has been made for the compliance of the load frame. The curves are intentionally off-set to show all results. Strain hardening values are given below, which are summarized in Table 6.

providing an additional improvement in resistance to irradiation embrittlement. TZM has an elongated, sheet-like grain structure with coarser grains, coarse carbide particles, and titanium + zirconium in solid solution. The coarse carbide particles with the higher carbon content may be limitations that result in poor resistance to irradiation embrittlement for TZM Mo with a 700 °C DBTT [42].

The brittle failure modes observed for LSR ODS Mo irradiated at 294 °C and 560–609 °C and then tested at temperatures below the DBTT were transgranular cleavage, which indicates that grain boundaries or

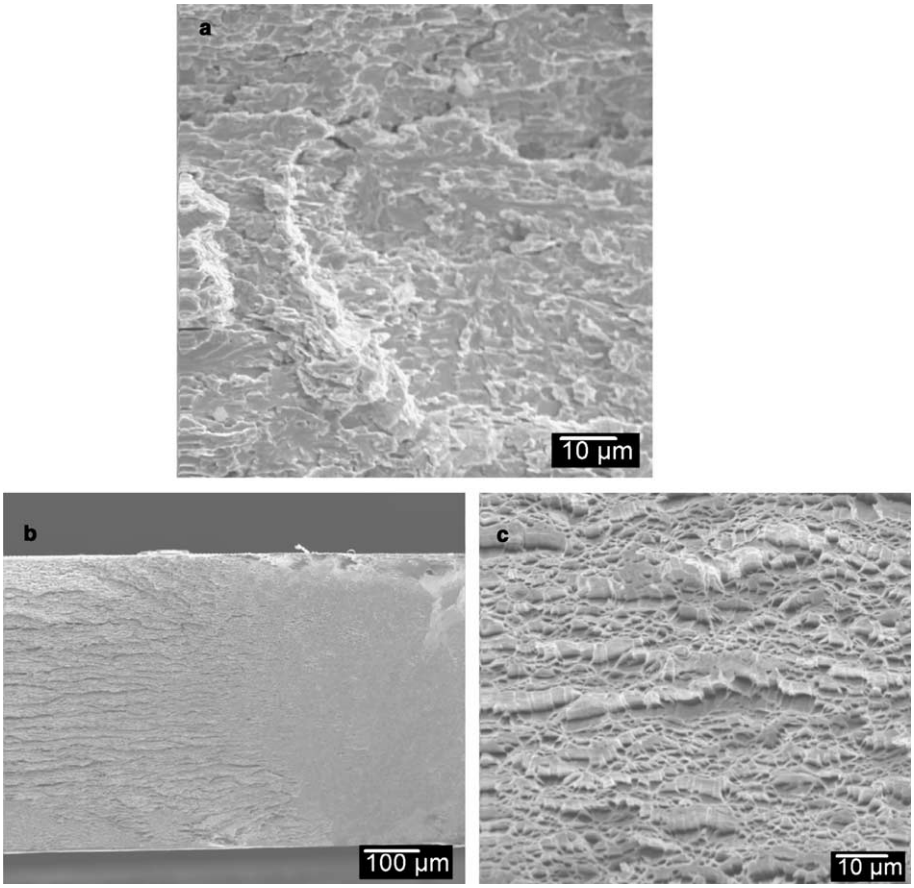

Fig. 6. Post-irradiated SEM fractography of ODS molybdenum following 294 °C irradiations to 23.2×10^{25} n/m^2 for tensile testing at: (a) room-temperature showing transgranular cleavage, (b) temperature of 600 °C showing mixed-mode fracture mode, and (c) temperature of 800 °C showing a ductile-laminate failure mode.

oxide interfaces were not the preferred fracture path and is similar to results observed for LCAC and TZM [7,42]. Small, linear defects that could be microcracks or grain boundaries were observed to be the fracture initiation sites at test temperatures below the DBTT for ODS Mo. The ductile laminate structure observed for both ODS and high-purity [24] molybdenum, where fracture initiation occurs at grain boundaries and oxide boundaries to leave fine ligaments that are pulled to failure under plane stress conditions to allow large amounts of fracture energy to be absorbed, likely plays a role in the enhanced resistance to irradiation embrittlement. The fine spacing of grains also provides closer spacing of grain boundaries that are neutral sinks for the point defects produced by irradiation, which could lower the number density and size of voids and loops, and reduce the effectiveness of these hardening barriers. The second benefit of the finer grain size is that the size of the ligaments (i.e. grains) formed during the fracture process is also reduced, which provides a more dominant plane stress-state that increases ligament plasticity.

Irradiation of molybdenum at 294 °C would be expected to result in the formation of a high number density of fine loops and voids [1,3,4,6,39,43] that limit dislocation motion and result in elevation of the effective yield stress above the inherent fracture stress of the material so that a brittle fracture stress is measured at temperatures below the 800 °C DBTT. However, the tensile strength values measured for 294 °C irradiated ODS molybdenum test at room-temperature to 600 °C, which are fracture stress values, are comparable to the yield strength values determined for the 560–609 °C irradiated LSR ODS Mo at temperatures above the DBTT where plastic deformation is observed. This coincidence of equivalent tensile strength values for the 294 °C and 560–609 °C irradiations could be explained by the fact that the cracking along grain boundaries that initiates the ductile laminate failure occurs at the same macroscopic stress level. Testing of non-irradiated molybde-

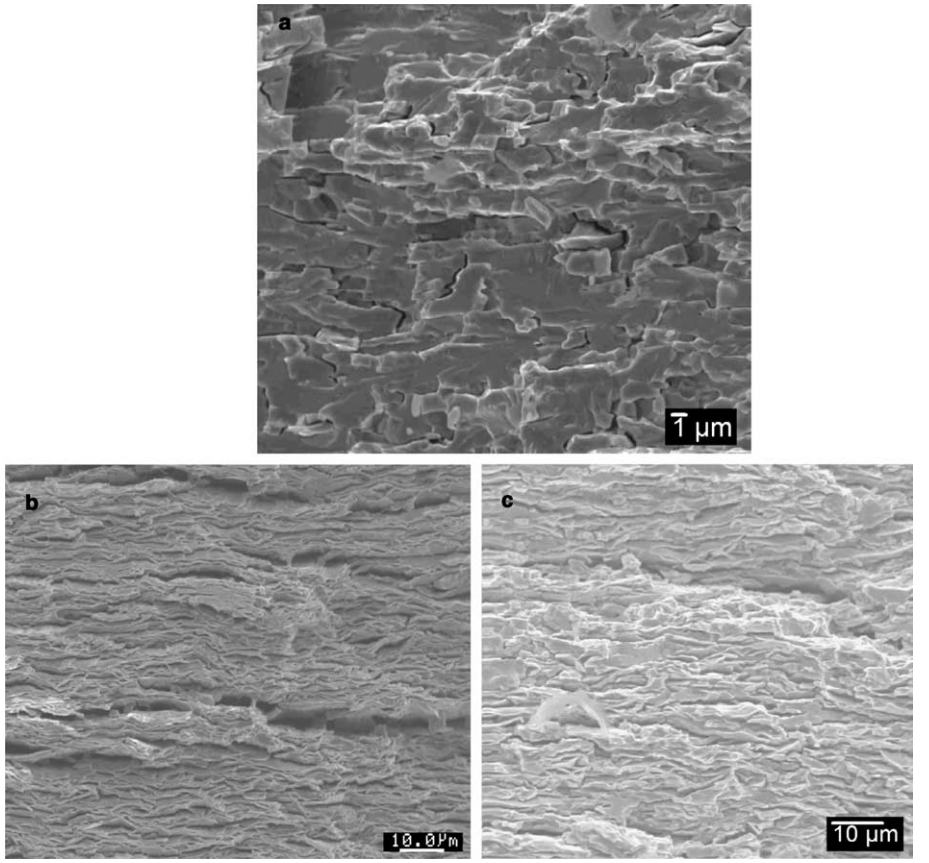

Fig. 7. Post-irradiated SEM fractography of LSR ODS molybdenum after irradiations at 560–609 °C for tensile testing at: (a) temperature of −50 °C after dose of 7.26×10^{25} n/m^2 showing brittle, transgranular fracture, (b) room-temperature after a dose of 7.26×10^{25} n/m^2 showing a ductile laminate failure mode, and (c) room-temperature after a dose of 24.6×10^{25} n/m^2 showing a ductile laminate failure mode.

num alloys has shown that the initiation of the ductile laminate failure mode by grain boundary micro-cracking occurs in the region of triaxial stresses [17,18]. The coarser voids that would be expected for the 560–609 °C irradiations of molybdenum [1,3,4,6,39,43] may not limit plasticity in the fine laminates under the plane stress conditions that precede this micro-cracking so that the ductile laminate failure mechanism occurs at much lower temperatures and macroscopic plasticity is observed with only a slight elevation of the DBTT. The high number density of fine dislocation loops and voids expected for the 294 °C irradiation may prevent the laminates from plastically deforming once cracks form on grain boundaries, and brittle fracture occurs by transgranular cleavage across grains. However, localized plastic events or necking which would result in the triaxial stress-state and lead to the grain boundary micro-cracking that produces the ductile-laminate fracture was not observed for irradiated ODS Mo. This may indicate that a triaxial stress-state may not be needed when ODS Mo is irradiation hardened. The finer grain size and oxide particle size of ODS Mo likely results in the formation of fine laminates and preliminary TEM examinations suggest that the size and number density of voids are reduced in this material, which allows the laminates to plastically deform more easily and results in resistance to irradiation embrittlement for 560–609 °C irradiated LSR ODS Mo. However, the strong temperature dependence for the tensile strength results for both 294 °C and 560–609 °C irradiated ODS Mo is difficult to explain, but could result from a strong temperature dependence for the stresses needed to initiate the ductile laminate failure mechanism. Depletion of point defects at grain boundaries and oxide interfaces would vary in effectiveness for the 294 °C and 560–609 °C irradiation temperature due to differences in point defect diffusion rates. More examinations of micro-structure are needed to determine how improved resistance to irradiation embrittlement is achieved for ODS Mo irradiated at 560–609 °C, but no improvement over results for LCAC and TZM is observed for the 294 °C irradiations.

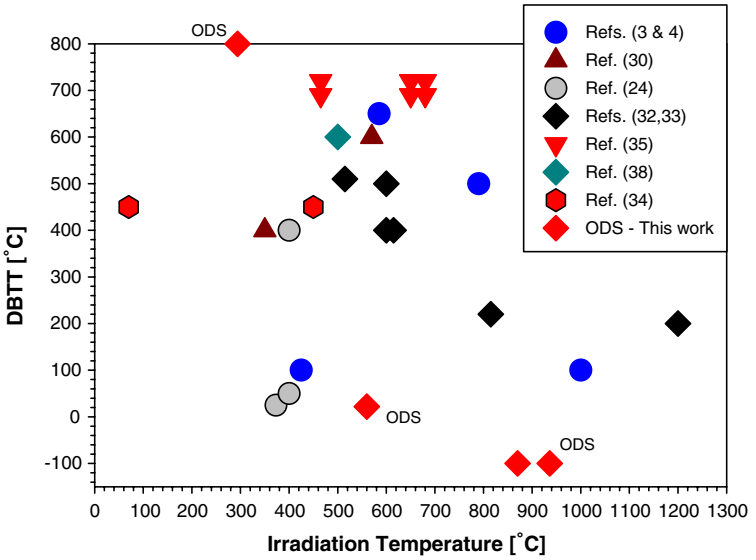

Fig. 8. Summary of results for ODS DBTT values obtained in this work compared with literature data for molybdenum as a function of irradiation temperature.

Table 7
Summary of calculated and measured irradiation hardening results with calculated fraction of void cutting (Eq. (4)) for ODS tensile data from 870 °C irradiations

Test temperature [°C]	Measured values			Calculated values		
	Irradiation temperature [°C]	Fluence [n/m^2], $E > 0.1$ MeV	Measured $\Delta\sigma_{YS}$ [MPa]	Orowan hardening, Eq. (1), [MPa]	Void cutting, Eq. (3), [MPa]	Fraction of voids cut, Eq. (4) $f_{V\text{-cut}}$
Longitudinal stress-relieved data						
−100	870	2.28×10^{25}	125	176	26.8	0.34
−50			192			N/A
22			94			0.55
22			108			0.46
982			−32			N/A
982			−25			N/A
−100		6.44×10^{25}	246	486	64.0	0.57
−50			314			0.41
22			180			0.73
22			276			0.50
982			120			0.87
982			120			0.87
Transverse stress-relieved data						
300	870	2.28×10^{25}	−4	176	26.8	N/A
300			−9			N/A
300		6.44×10^{25}	152	486	64.0	0.79
300			196			0.69

Notes: 1. The void size and number density data used for the calculations were taken from TEM characterization of the same material reported in literature [29]. 2. For 870 °C irradiations at a dose of 2.28×10^{25} n/m^2, the average void size was 50 nm with a nominal number density of 1.4×10^{20} #/m^3. For the 870 °C irradiations at a dose of 6.44×10^{25} n/m^2, the average void size was 20 nm with a nominal number density of 1.7×10^{20} #/m^3. 3. Measured irradiation hardening ($\Delta\sigma_{YS}$) was determined by subtracting the post-irradiated and non-irradiated yield strength values.

3.2.2. Results for transverse stress-relieved (TSR) ODS

One tensile test was performed at room-temperature on TSR ODS Mo that was irradiated at 609 °C to a lower dose of 7.26×10^{25} n/m^2, and nil ductility, linear–elastic behavior in the load–displacement curve, and a brittle failure mode of transgranular cleavage was observed. This indicates that the tensile DBTT for 609 °C irradiated TSR ODS Mo is above room-temperature. Since the starting tensile DBTT for non-irradiated TSR ODS Mo is room-temperature, an increase in DBTT above room-temperature following the 600 °C irradiations is not surprising, and shows the anisotropy in tensile properties of ODS molybdenum.

3.3. Post-irradiation tensile properties for irradiation at 870 °C and 936 °C

3.3.1. Results for longitudinal stress-relieved (LSR) ODS

Heat treatment of LSR ODS Mo in high vacuum ($<6 \times 10^{-5}$ MPa) at 1000 °C for 1812 h, which is comparable to the exposure time for the 6.44×10^{25} n/m^2 (3.4 dpa-Mo) dose irradiations, resulted in no change

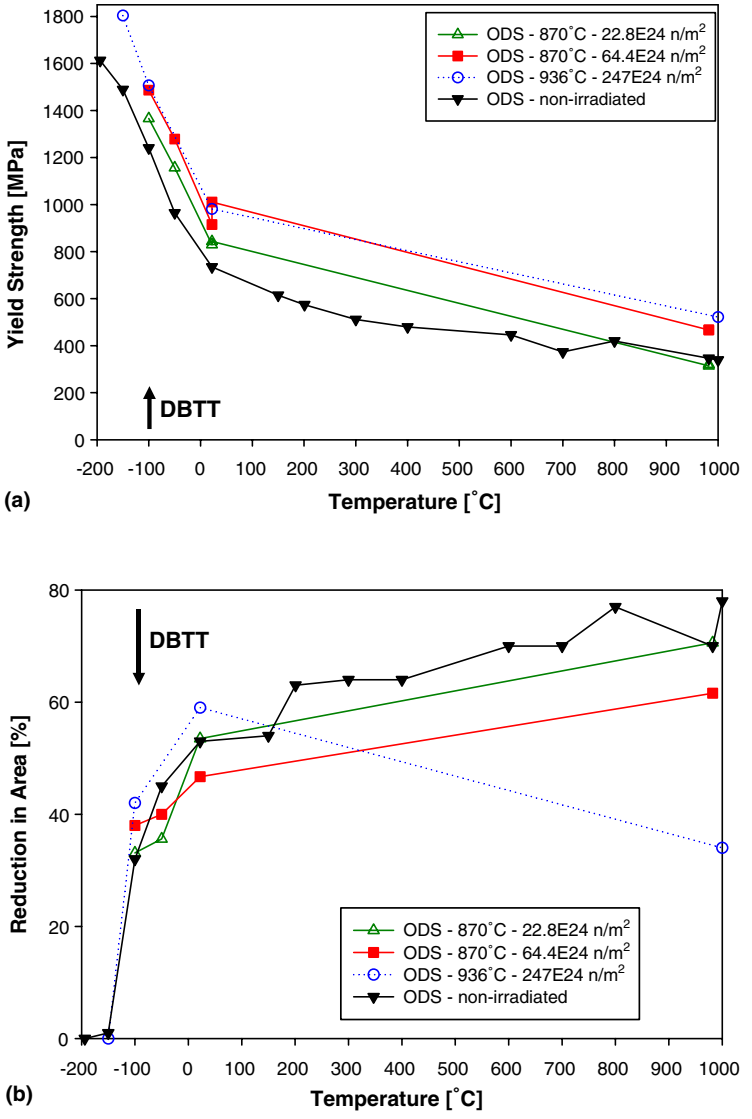

Fig. 9. Comparison of non-irradiated and post-irradiated tensile properties for LSR ODS molybdenum irradiated at 870 °C and 936 °C to fluences of 2.28, 6.44, and 24.7×10^{25} n/m^2 (corresponds to Mo-dpa values of 1.2, 3.4, and 13.1, respectively): (a) yield strength values, and (b) reduction in area values. The yield strength values determined at temperatures below the DBTT are actually a fracture stress in some cases as true plastic deformation has not been achieved.

in tensile properties, which is consistent with the high recrystallization temperature of 1700 °C for a 1-h heat treatment for ODS Mo. Recrystallization of ODS Mo was not observed during the irradiations, and a low number density of coarse voids with no dislocation loops have been reported for the 870 °C irradiations of the same material [29] (see Table 7). The formation of a low number density of coarse voids results in relatively small increases in tensile strength (10–34% increase in yield strength) at test temperatures of −150 °C to room-temperature with low amounts of irradiation hardening (see Fig. 9). The tensile strength of LSR ODS Mo irradiated at 870 °C to a lower dose of 2.28×10^{25} n/m^2 (1.2 dpa) was only slightly higher than the non-irradiated values, while slightly higher tensile results were observed at the higher dose of 6.44×10^{25} n/m^2 (3.4 dpa). The tensile strength values for ODS Mo irradiated at 936 °C to the highest dose of 24.7×10^{25} n/m^2 (13.1 dpa) were comparable to tensile strength values for the 870 °C irradiations to the dose of 6.44×10^{25} n/m^2. Only small differences in the size and number density of voids would be expected for the 870 °C and 936 °C irradiation of ODS molybdenum that would be expected to result in insignificant differences in tensile strength [1,4,39,43,49]. The similarity in tensile strength results for the 870 °C/6.44×10^{25} n/m^2 and 936 °C/24.7×10^{25} n/m^2 irradiations indicates that the void sizes and number densities are fairly similar, and saturation of the increase in tensile strength for irradiations of ODS Mo at temperatures ranging from 870 °C to 936 °C occurs at a dose of 6.44×10^{25} n/m^2 or lower. This is similar to the 7.33×10^{25} n/m^2 dose needed for saturation of the increase in yield strength observed for 936 °C irradiated TZM with increases in yield strength (13–36%) close to that observed for LSR ODS Mo [42].

The hardening from the voids for the 870 °C irradiations of ODS molybdenum can be calculated using a form of classical Orowan (σ_{OR}) hardening [43,49,50]:

$$\sigma_{OR} = (2Gb)/l_V, \quad (1)$$

where G is the shear modulus, b is the Burgers vector, and l_V is the spacing of the voids, which is determined from the following for an ordered distribution,

$$l_V = 1/(d_v N_v)^{1/2}, \quad (2)$$

where d_v is the void diameter and N_v is the number density of voids. The Orowan stress represents the largest possible resistance to dislocation motion for an ordered array of voids, while a random array of voids can result in Orowan hardening values that are 20% less. If the

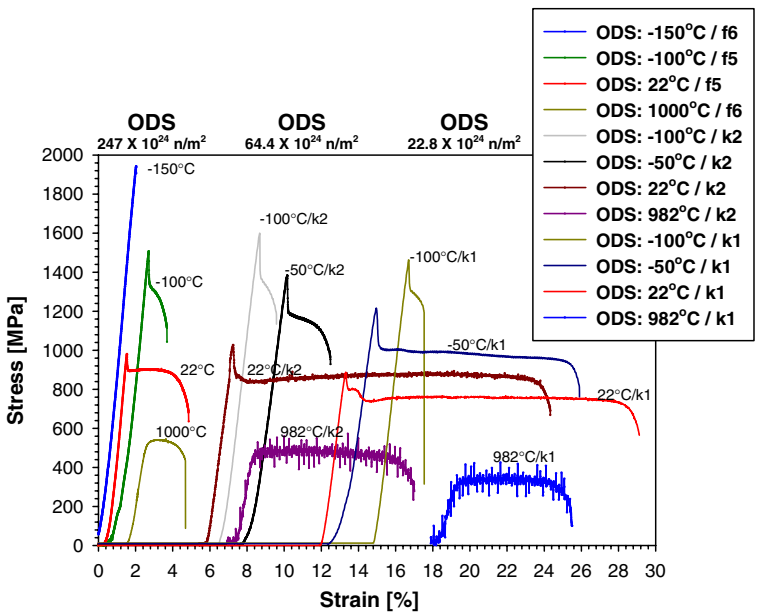

Capsule	f6	f5	f5	f6	k2				k1			
Test Temp	-150°C	-100°C	22°C	1000°C	-100°C	-50°C	22°C	982°C	-100°C	-50°C	22°C	982°C
n	--	-0.61	0.025	0.15	-0.40	-0.21	0.082	0.022	-0.26	0.014	0.048	0.006

Fig. 10. Plot of load–displacement curves for LSR ODS molybdenum from tensile testing at temperatures of −150 °C to 1000 °C following irradiation at 870–936 °C to a fluence of either 24.7×10^{25} n/m^2 (f5 and f6), 6.44×10^{25} n/m^2 (k2), or 2.28×10^{25} n/m^2 (k1). The stress–strain data were determined from the raw load–displacement results, and no correction was made for the compliance of the load frame. Strain hardening values are given below, and are summarized in Table 6.

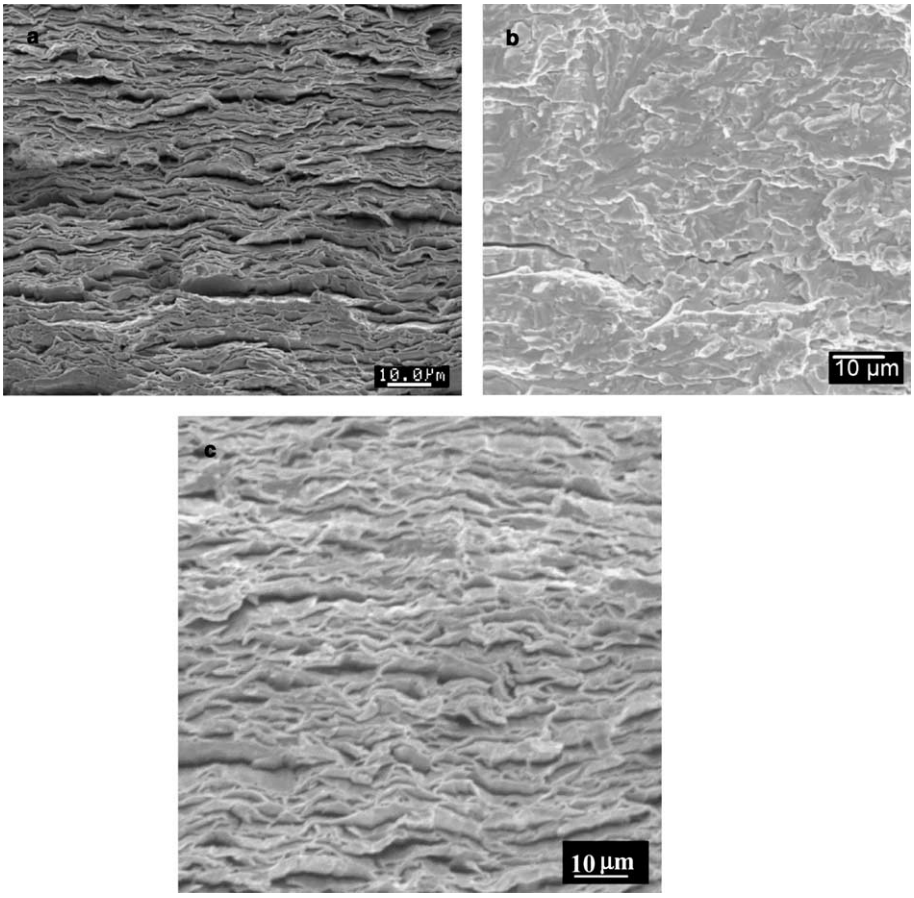

Fig. 11. Post-irradiated SEM fractography of LSR ODS molybdenum following irradiations at 870 °C and 936 °C to for tensile testing of: (a) ODS irradiated at 870 °C to dose of 6.44×10^{25} n/m^2 and then tested at −100 °C, (b) ODS irradiated at 936 °C to dose of 24.7×10^{25} n/m^2 and then tested at −150 °C, and (c) ODS irradiated at 936 °C to dose of 24.7×10^{25} n/m^2 and then tested at −100 °C.

dislocations are able to cut through the voids, then the irradiation hardening (σ_{SV}) is expressed as [50]:

$$\sigma_{SV} = (Gb/l_V)(\ln(R_v/r_d)/2\pi), \quad (3)$$

where R_v is the radius of the void and r_d is the radius of the dislocation core, which is assumed to be twice the burgers vector (5.46 Å). The calculated void hardening values for the voids acting as hard barriers (Eq. (1)) are shown in Table 7 to be much larger than the measured irradiation hardening, while the irradiation hardening for dislocations cutting the voids (Eq. (3)) was much lower than the measured value. Assuming that some fraction of the voids are cut by the dislocations ($f_{V\text{-cut}}$), the calculated values (σ_{CAL}) can be fit to the measured radiation hardening values by varying the fraction of voids that are cut by dislocations (Table 7):

$$\sigma_{CAL} = (\sigma_{OR}(1 - f_{V\text{-cut}})) + (\sigma_{SV} f_{V\text{-cut}}). \quad (4)$$

An exact match between measured and calculated irradiation hardening would be observed if the fraction of void cutting varies from 0.34 to 0.87, and this fraction can vary with test temperature. However, the cutting of voids by dislocations was not previously resolved [29] so there is some question if this mechanism is observed. However, these results do indicate that the low irradiation hardening observed for 870–936 °C irradiated LSR ODS Mo results from the low number density of coarse voids that are formed at this irradiation temperature.

The stress–strain curves for 870–936 °C irradiated LSR ODS Mo are shown in Fig. 10 to be generally similar to non-irradiated material (Fig. 2) with the notable exception of a higher upper/lower yield point (Lüder's plateau), the Lüder's plateau occurring over a smaller displacement range, and slightly lower strain-hardening exponents for tensile testing of irradiated material at room-temperature to −100 °C. The higher upper/lower yield point indicates that the formation of coarse voids during the 870–936 °C irradiations results in a slight increase in the stresses needed to initiate dislocation motion. The slightly lower strain hardening exponents for 870–936 °C irradiated ODS Mo compared to

non-irradiated material indicates that the low number density of coarse voids have only a small effect on the plastic flow properties. Tensile testing of 870–936 °C irradiated ODS Mo at 1000 °C shows that the strain hardening and tensile strength values are larger than non-irradiated material tested at 1000 °C by a greater percentage than observed for testing at lower temperatures, which suggests that the void structure formed by the 870–936 °C irradiations is stable up to temperatures of 1000 °C.

Large amounts of tensile ductility, plasticity in the load–displacement curves (Fig. 10), and ductile failure modes were observed for 870 °C irradiated LSR ODS Mo following tensile testing at temperatures ranging from −100 °C to 1000 °C. The ductile laminate failure mode observed at −100 °C for LSR ODS Mo irradiated at 870 °C to doses of 2.28 and 6.44×10^{25} n/m^2 is shown in Fig. 11(a) to be similar to that observed at −100 °C for non-irradiated material (Fig. 3(a)). Similarly, high tensile ductility, plasticity in the load–displacement curves and a ductile laminate failure (Fig. 11(c)) similar to non-irradiated material were observed for 936 °C/24.7×10^{25} n/m^2 dose irradiated LSR ODS Mo when tested at −100 °C. Very low tensile ductility, linear–elastic behavior in the load–displacement curve, and a brittle fracture mode consisting of transgranular cleavage (Fig. 11(b)) comparable to non-irradiated material (Fig. 3(b)) was observed at −150 °C. These results indicate that the DBTT of 870–936 °C irradiated LSR ODS Mo was higher than −150 °C and less than −100 °C, but is conservatively defined as −100 °C (Table 5). This represents no change in the DBTT of LSR ODS Mo following irradiation at 870–936 °C to doses as high as 24.7×10^{25} n/m^2.

Similar levels of irradiation hardening with no change in DBTT were observed for both 870–936 °C irradiated LSR ODS Mo and 936 °C irradiated TZM Mo [42] at a dose of 24.7×10^{25} n/m^2 with effective saturation of properties for both alloys at a dose between 6.44 and 7.33×10^{25} n/m^2. Both ODS and TZM Mo are resistant to grain growth and recrystallization during long-term exposures at 1000 °C, which results in small amounts of hardening from the formation of coarse voids but no change in DBTT. Recrystallization of LSR LCAC during the 936 °C irradiations results in a small decrease in tensile strength at lower doses followed by hardening with the net result of no change in tensile strength relative to non-irradiated LSR LCAC Mo [42]. However, the increase in grain size during the 936 °C irradiations of LSR LCAC Mo results in an increase in DBTT from −100 °C to −50 °C. Use of molybdenum alloys that are micro-structurally stable at high temperatures, such as ODS, TZM, and recrystallized LCAC, is most desired for irradiations at 870–1000 °C. The DBTT for 870–936 °C irradiated LSR ODS Mo is shown in Fig. 8 to be much lower than reported in literature or for TZM and LCAC, see Table 5. The fine grain size of ODS and micro-structural stability afforded by the presence of the oxide particles results in the lowest DBTT for a molybdenum alloy irradiated at 870–936 °C.

3.3.2. Results for transverse stress-relieved (TSR) ODS

Limited tensile testing of 870 °C irradiated TSR ODS at 300 °C to doses of 2.28×10^{25} n/m^2 and 6.44×10^{25} n/m^2 produced results showing increases in yield strength (−2% to 38%) comparable to LSR ODS (Table 6) with the tensile ductility and ductile failure modes comparable to non-irradiated material. Although this testing cannot be used to determine if a change in DBTT had been reached for TSR ODS Mo, the similarity in irradiation hardening and high amounts of tensile ductility indicates that the change in tensile properties for 870–936 °C irradiated TSR and LSR ODS Mo are similar, which is the same result previously reported for 1100 °C irradiated LCAC [7].

4. Summary

Irradiation of ODS Mo at 294 °C and 560–609 °C to high fluences of 12.3–13.1 dpa results in large increases in tensile strength (57–173%), but the strong temperature dependence in post-irradiated tensile results was notably different than observed for other molybdenum alloys such as TZM and LCAC. The DBTT for 294 °C irradiated LSR ODS Mo was determined to be 800 °C, which is the same as that observed for LCAC and TZM Mo irradiated at 294 °C to the same dose. However, the DBTT for 560–609 °C irradiated LSR ODS Mo was determined to be room-temperature, which is a significant improvement over the DBTT values determined for LCAC (300 °C) and TZM (700 °C), and literature data for 600 °C irradiations (DBTT = 100–700 °C). ODS Mo had a fine grained micro-structure with elongated, pancaked grains produced by wrought processing, which indicates that this micro-structural feature, with the presence of fine oxide particles, may provide enhanced resistance to irradiation embrittlement.

ODS Mo exhibited a ductile-laminate failure mode where the fracture starts by the formation of micro-cracks on boundaries that leave ligaments of sheet-like grains that are then stretched to failure under plane stress conditions with a high degree of plasticity. The fine grained, elongated pancaked grain structure of ODS Mo likely provides two major benefits: (1) reduces the size of ductile laminate features formed at the fracture surface so that a plane stress-state more conducive to a large extent of plastic deformation can be produced when the material is irradiation hardened, and (2) reduces the spacing of boundaries that are neutral sinks

for point defects and potentially reduces the number density of loops and voids that are barriers for the dislocation motion needed for plastic deformation of the laminates. However, the tensile strength values determined for the 294 °C irradiations at room-temperature to 600 °C, which are a fracture stress because brittle failure is observed, are comparable to yield strength results for the 560–609 °C irradiations where plasticity is observed, which could indicate that the stress required to initiate the intergranular cracking that leads to the ductile laminate failure mode is the same for both irradiated conditions. Irradiation at 294 °C is expected to produce a higher number density of smaller loops and voids that may prevent plastic deformation of the laminates and result in a brittle failure mode at much higher test temperatures. Irradiation of ODS Mo at 560–609 °C is expected to produce a lower number density of coarser voids and a very low loop density so that plastic deformation of the fine laminates can occur at lower temperatures to result in a lower DBTT. However, more detailed examinations of micro-structure are needed to determine how resistance to irradiation embirttlement is observed for 560–609 °C irradiated ODS Mo, while no improvement in irradiation embrittlement is observed for 294 °C irradiations.

Irradiation of LSR ODS Mo at 870–936 °C results in small increases in yield strength (10–34%) that are saturated at or before a dose of 6.44×10^{25} n/m^2 with no change in yield strength out to a dose of 24.7×10^{25} n/m^2. No change in DBTT was observed for 870–936 °C irradiated LSR ODS Mo relative to non-irradiated material with a post-irradiation DBTT of −100 °C observed at fluences between 2.28 and 24.7×10^{25} n/m^2. Irradiation of molybdenum alloys at temperatures > 800 °C results in the formation of a low number density of coarse voids that are shown to have little effect on the tensile properties. The fine grain size of LSR ODS Mo and the micro-structural stability afforded by the presence of the oxide particles results in the lowest DBTT reported for a molybdenum alloy irradiated at 870–936 °C.

Acknowledgments

This work was supported under USDOE Contract No. DE-AC11-98PN38206. Thanks to the following ORNL personnel for completing the irradiations, tensile testing and fractography (J.P. Strizak, T.S. Byun, A.L. Qualls, A.W. Williams, and J.L. Bailey).

References

[1] V.K. Sikka, J. Moteff, Nucl. Technol. 22 (1974) 52.
[2] S.J. Zinkle, N.M. Ghoniem, Fus. Eng. Des. 51&52 (2000) 55.
[3] B.L. Cox, F.W. Wiffen, J. Nucl. Mater. 85&86 (1979) 901.
[4] F.W. Wiffen, in: R.J. Arsenault (Ed.), Proceedings of the 1973 International Conference on Defects and Defect Clusters in B.C.C. Metals and Their Alloys, Nucl. Metall. 18 (1973) 176.
[5] R.E. Gold, D.L. Harrod, J. Nucl. Mater. 85&86 (1979) 805.
[6] B.N. Singh et al., J. Nucl. Mater. 212–215 (1994) 1292.
[7] B.V. Cockeram, J.L. Hollenbeck, L.L. Snead, J. Nucl. Mater. 324 (2004) 77.
[8] M. Semchyshen, R.Q. Barr, J. Less Common Met. 11 (1966) 1.
[9] J. Wadsworth, T.G. Nieh, J.J. Stephens, Scr. Metall. 20 (1986) 637.
[10] Standard Specification for Molybdenum and Molybdenum Alloy Plate, Sheet, Strip, and Foil, ASTM B386-97, American Society for Testing and Materials, Philadelphia, PA, 1997.
[11] J.B. Lambert, J.J. Rausch, Non-Ferrous Alloys and Special-Purpose Materials, Materials Handbook, vol. 2, ASM International, Materials Park, OH, 1992, p. 557.
[12] J. Wadsworth, C.M. Packer, P.M. Chewey, W.C. Coons, Metall. Trans. 15A (1984) 1741.
[13] R. Bianco, R.W. Buckman Jr., C.B. Geller, US Patent #5,868,876, 9 February 1999.
[14] A.J. Mueller, J.A. Shields, R.W. Buckman Jr., in: G. Kneringer, P. Rodhammer, H. Wildner (Eds.), Proceedings 15th International Plansee Seminar, vol. 1, Plansee Holding AG, Reutte, Austria, 2001, p. 485.
[15] R. Bianco, R.W. Buckman Jr., 1995 Spring ASM/TMS Symposium on High Temperature Materials, May 19, 1995, GE CR&D Center, Schenectady, NY, Available as WAPD-T-3073, DOE/OSTI, Oak Ridge, TN, 1995.
[16] R. Bianco, R.W. Buckman Jr., in: A. Crowson, E.S. Chen, J.A. Shields, P.R. Subramanian (Eds.), Molybdenum and Molybdenum Alloys, The Minerals, Metals and Materials Society, Warrendale, PA, 1998, p. 125.
[17] B.V. Cockeram, Metall. Trans. 33A (2002) 3685.
[18] B.V. Cockeram, Metall. Trans. 36A (2005) 1777.
[19] A. Kumar, B.L. Eyre, Proc. R. Soc. London A370 (1980) 431.
[20] H. Kurishita, H. Yoshinaga, Mater. Forum 13 (1989) 161.
[21] W.D. Klopp, J. Less Common Met. 42 (1975) 261.
[22] A. Lawley, J. Van den Sype, R. Maddin, J. Inst. Met. 91 (1962-1963) 23.
[23] B.V. Cockeram, J.L. Hollenbeck, L.L. Snead, J. Nucl. Mater. 336 (2005) 299.
[24] A. Hasegawa et al., J. Nucl. Mater. 233–237 (1996) 565.
[25] L.L. Snead, S.J. Zinkle, Nucl. Instrum. and Meth. B 191 (2002) 497.
[26] L.R. Greenwood, F.A. Garner, J. Nucl. Mater. 212–215 (1994) 635.
[27] Standard Test Methods for Tension Testing of Metallic Materials, ASTM E8-01, American Society for Testing and Materials, Philadelphia, PA, 2001.
[28] L.R. Greenwood, R.K. Smither, Specter: Neutron Damage Calculations for Materials Irradiations ANL/FPP/TM-197, Argonne National Laboratory, January, 1985.
[29] R. Baranwal, M.G. Burke, Transmission electron microscopy of oxide dispersion strengthened (ODS) molybdenum: effects of irradiation on material structure, in: Proceedings

of Microstructural Processes in Irradiated Materials, San Diego, CA, March 2003, TMS, 2004, Available as B-T-3462, DOE/OSTI, Oak Ridge, TN, 2003.
[30] K. Watanabe et al., J. Nucl. Mater. 258–263 (1998) 848.
[31] V. Chakin, V. Kazakov, J. Nucl. Mater. 233–237 (1996) 570.
[32] K. Abe et al., J. Nucl. Mater. 122&123 (1984) 671.
[33] K. Abe et al., J. Nucl. Mater. 99 (1981) 25.
[34] M. Scibetta, R. Chaouadi, J.L. Puzzolante, J. Nucl. Mater. 283–287 (2000) 455.
[35] T. H. Webster, et al., in: Proceedings of BNES Conference on Irradiation Embrittlement and Creep in Fuel Cladding and Core Components, 9–10 November 1972, p. 61.
[36] I.V. Gorynin et al., J. Nucl. Mater. 191–194 (1992) 421.
[37] A. Hasegawa et al., J. Nucl. Mater. 225 (1995) 259.
[38] H.H. Smith, D.J. Michel, J. Nucl. Mater. 66 (1977) 125.
[39] K. Furuya, J. Moteff, Metall. Trans. 12A (July) (1981) 1303.
[40] K.S. Chan, Metall. Trans. 20A (1989) 155.
[41] K.S. Chan, Metall. Trans. 20A (1989) 2337.
[42] B.V. Cockeram, R.W. Smith, L.L. Snead, J. Nucl. Mater., this issue, doi:10.1016/j.jnucmat.2005.06.016.
[43] V.K. Sikka, J. Moteff, J. Nucl. Mater. 54 (1974) 325.
[44] J.A. Sprague et al., J. Nucl. Mater. 85&86 (1979) 739.
[45] T.S. Byun, K. Farrell, N. Hashimoto, J. Nucl. Mater. 329–333 (2004) 998.
[46] M.S. Wechsler, The Inhomogeneity of Plastic Deformation, American Society for Metals, 1971 (Chapter 2).
[47] A. Luft, Prog. Mater. Sci. 35 (1991) 97.
[48] K. Furuya, J. Moteff, J. Nucl. Mater. 99 (1981) 306.
[49] J. Moteff, D.J. Michel, V.K. Sikka, in: R.J. Arsenault (Ed.), Proceedings of the 1973 International Conference on Defects and Defect Clusters in B.C.C. Metals and their alloys, Nucl. Metall. 18 (1973) 176.
[50] D.R. Olander, Fundamental Aspects of Nuclear Reactor Fuel Elements, Technical Information Center, US-DOE, ERDA 1976 (TID 2671).